

Structure and stability of quasicrystals: Modulated tiling models

M. Krajčí* and J. Hafner

Institut für Theoretische Physik, Technische Universität Wien, Wiedner Hauptstrasse 8-10, A-1040 Wien, Austria

(Received 24 February 1992)

A modulated tiling model for the structure of an icosahedral quasicrystal of the Al-Zn-Mg class is proposed. Idealized structure models for quasicrystals are constructed on the basis of three-dimensional Penrose tilings with a Henley-Elser decoration of the basic structural units. The stability of these structures is investigated by an isothermal molecular-dynamics annealing of a hierarchy of crystalline approximants to the quasiperiodic structure, based on realistic pair forces derived from pseudopotential theory. We find that quasicrystals are stable only at compositions leading to an electron-per-atom ratio of $e/A \approx 2.1-2.2$, thus confirming the existence of a Hume-Rothery or Peierls mechanism for the stability of quasicrystals. Because of the large number of different atomic environments in quasicrystals, any set of interatomic forces leads to a displacive modulation of the idealized quasiperiodic structure. For a stable quasicrystal, the displacement field has the symmetry of the quasilattice. The structural characteristics of the displacively modulated Penrose tilings are investigated in detail. We show that the modulation of the structure substantially improves the agreement of the models with experimental observation.

I. INTRODUCTION

Since the discovery of quasicrystalline alloys by Shechtman *et al.*¹ theoretical investigations have focused on the structure of these materials. It has been shown that these alloys share two characteristics: the diffraction patterns can be indexed using the set of basis vectors appropriate to an icosahedral quasilattice, and nearly all exhibit a significant degree of disorder signaled by broadened diffraction peaks. Several structural models that account for the gross features of the diffraction patterns from icosahedral alloys have been proposed. Quasiperiodic descriptions such as the three-dimensional Penrose tiling² and the icosahedral glass model^{3,4} both yield scattering functions with icosahedral symmetry. A relatively large degree of disorder is intrinsic to the icosahedral glass model. The Penrose tiling also produces broadened diffraction peaks, if modified by the inclusion of a random phason strain⁵ (the phason momentum describes a degree of freedom that appears due to the fundamental incommensurability of the quasiperiodic lattice).

Another important open question is why nature should prefer quasiperiodic to periodic order. A phenomenological approach to this problem is based on Landau-type expansions of the free energy in powers of the Fourier components $\rho(\mathbf{q})$ of the mass density.⁶⁻⁸ It was found that stable quasiperiodic solutions may exist. Microscopic treatments are based mostly on computer simulations. For example, Lançon and Billard^{9,10} and Sasajima *et al.*¹¹ found that a two-dimensional Penrose pattern is unstable under Lennard-Jones forces and relaxes to a hexagonal network. However, a Penrose-tiling decorated with two different types of atoms and Johnson-type potentials was found to be stable at sufficiently low temperatures.^{9,10} A similar result was obtained by Widom *et al.*¹² in Monte Carlo simulations of two-

dimensional binary quasicrystals. Special types of pentagonal and dodecagonal lattices were investigated by Jansen¹³ and Leung *et al.*¹⁴ Jansen also drew attention to the fact that the relaxation introduces a displacive modulation of the quasiperiodic tiling.

For three-dimensional systems Szebo and Villain¹⁵ showed that a hard-sphere model does not have quasiperiodic solutions for the ground state. On the other hand, Burkov and Levitov¹⁶ proved that under certain conditions the ground state of an n -dimensional lattice with codimension 1 can be quasicrystalline if the interactions are long ranged enough. Computer simulations of three-dimensional Penrose tilings with Lennard-Jones forces have been presented by Lançon and Billard¹⁰ and by Roth *et al.*¹⁷ It was found that when all vertices of a Penrose tiling are occupied by atoms, the system relaxes to a glassy state. However, if certain vertices are left vacant according to the unit-sphere packing of Henley,¹⁸ even a monoatomic quasicrystal is metastable.

Stability or metastability of quasicrystals has also been discussed from an electronic point of view. It has been pointed out that the stoichiometry of many quasicrystalline alloys appears to be governed by a Hume-Rothery rule, placing the Fermi surface near an effective Brillouin-zone boundary.¹⁹⁻²³ The existence of a strong electron-lattice interaction was confirmed through band-structure calculations for rational approximants to quasicrystals that demonstrate that the Fermi level is indeed in or near a minimum in the electronic density of states.²⁴⁻²⁷

A link between arguments based on the calculation of the electronic ground-state energy and computer simulations based on classical pair interactions is based on modeling studies based on interatomic forces derived from quantum theory.²⁸⁻³⁰ These investigations extended earlier work on the relation between trends in the interatomic forces and trends in the crystalline^{31,32} and

liquid³³ structures to quasicrystalline alloys. In metallic systems, the form of the interatomic potentials close to near-neighbor distances is determined by the interplay of a short-range screened Coulomb repulsion and a long-ranged oscillatory potential whose wavelength is given by $\lambda_F = 2\pi/2k_F$ (where k_F is Fermi momentum). A given crystal structure is stable if the periodicity of the lattice matches the Friedel wavelength λ_F —this condition is precisely the same as that for the occurrence of a Hume-Rothery or Peierls pseudogap at the Fermi level. Hafner and Heine³¹ had shown that, in a parameter space spanned by the ion valence Z , the atomic volume Ω , and the “core-radius” r_c (the one parameter characterizing the electron-ion pseudopotential) close-packed crystal structures with high coordination numbers ($N_c \geq 10$) and “open” structures with low coordination numbers ($N_c \leq 7$) are neatly separated. Smith³⁰ was the first to point out that in a narrow stripe separating open- and close-packed structures, a quasicrystalline structure may be lower in energy than any crystalline lattice (see also Ref. 34). Although no element falls into this region of parameter space, the virtual-crystal parameters of many quasicrystalline simple-metal alloys fall very close to the region of predicted quasicrystalline stability.

In this paper we extend the simulation studies to realistic models of icosahedral alloys, at the example of quasicrystalline Al-Zn-Mg alloys. An idealized structural model is constructed by a three-dimensional Penrose tiling, decorated as proposed by Henley and Elser.^{18,35} Interatomic potentials are calculated by pseudopotential perturbation theory, based on *ab initio* orthogonal-plane-wave pseudopotentials.³² Molecular-dynamics studies are performed for a series of rational approximants to the quasicrystalline lattice, with up to about 12 000 atoms in the periodically repeated cell. Our molecular-dynamics simulations show that the quasicrystalline structures are metastable only at the stoichiometry leading to an electron-per-atom ratio in accordance with a generalized Hume-Rothery rule. The relaxation of the idealized structure under realistic pair forces leads to a displacive modulation of the quasicrystalline structure. The effect of the molecular-dynamics annealing on the pair correlation functions, bond-angle correlation functions, and powder and Bragg diffraction patterns is studied in detail. We show that the displacive modulation of the idealized structure greatly improves the agreement with experiment. We conclude that a computer-relaxed Penrose tiling with a Henley-Elser decoration yields a very accurate description of the structure and stability of icosahedral Al-Zn-Mg alloys and a reliable starting point for theoretical studies of the electronic and vibrational properties. Some of our results have been discussed very briefly in a previous paper.²⁹

II. QUASICRYSTAL AND CRYSTALLINE APPROXIMANTS

Henley and Elser³⁵ have proposed a model for Al-Zn-Mg-type icosahedral quasicrystals based on the assumption that the structural framework of the icosahedral

phases is the three-dimensional (3D) Penrose tiling. An atomic decoration of the Penrose lattice is derived from the crystal structure³⁶ of the Frank-Kasper phase (Al,Zn)₄₉Mg₃₂.

The 3D Penrose lattice can be generated either by the dual method,^{37–39} or by the projection method.⁴⁰ The projection method is based on projecting a “strip” of a six-dimensional (6D) hypercubic lattice L_6 onto the 3D physical space E_3 . The strip is defined by extending a unit cube in L_6 parallel to E_3 . The orientation of E_3 is defined in such a way that the projection of a star of orthogonal basis vectors in L_6 forms an icosahedral basis in E_3 , $\mathbf{e}_l = C(0, 1, \tau) +$ cyclic permutations (c.p.): $l = 1, 2, 3$; $\mathbf{e}_l = C(0, -1, \tau) +$ c.p., $l = 4, 5, 6$, where $\tau = (1 + \sqrt{5})/2$ is the golden mean, C is a constant normalizing the basis vectors to unity. The projection of the 6D unit cube onto a 3D space E'_3 perpendicular to E_3 is a rhombic triacontahedron, the acceptance domain for vertices of the quasilattice. A vertex of L_6 belongs to the quasilattice only if its projection onto E'_3 falls into the acceptance domain.

The lattice of the crystalline approximants is obtained if, in the icosahedral basis in E'_3 , $\mathbf{e}'_l = C'(0, -\tau, -1) +$ c.p.: $l = 1, 2, 3$; $\mathbf{e}'_l = C'(0, \tau, 1) +$ c.p., $l = 4, 5, 6$, the golden mean τ is replaced by a rational number $\tau_n = F_{n+1}/F_n$, where the F_n are Fibonacci numbers, $F_0 = 0$, $F_1 = 1$, $F_{n+1} = F_n + F_{n-1}$. The icosahedral basis in E_3 is unchanged. The form of the acceptance domain in E'_3 , the rhombic triacontahedron

$$D = \left\{ \mathbf{t} + \sum_l x_l \mathbf{e}'_l, -0.5 \leq x_l \leq 0.5 \right\}, \quad (1)$$

is deformed for crystalline approximants, but its topology is conserved. The lattice created by this projection is a periodic Penrose lattice (PPL). It can be viewed as a tiling of two kinds of golden rhombohedra: prolate (PR) and oblate (OR) ones. The lattice has cubic symmetry. The period of the cubic symmetry is

$$a_n = \sqrt{(2 + 2/\sqrt{5})\tau^n} a_R, \quad (2)$$

where a_R is the length of the rhombohedron edge. The number of constituent rhombohedra, $N_R = 4F_{3n+3}$, increases with increasing order n of the approximant. We shall denote the approximants by F_{n+1}/F_n , the pair of Fibonacci numbers corresponding to the approximation τ_n to the golden mean τ .

Even if the form of the acceptance domain D is fixed, there are additional degrees of freedom associated with a shift \mathbf{t} of D in the space E'_3 (Ref. 41). The shift of the acceptance domain changes the configuration of the basic structural units of PPL (PR's and OR's) but not their relative frequencies. For each approximant there exists a periodically repeated cubic zone Z of nonequivalent shifts in E'_3 . The edge of this cubic zone has a length of $z = 1/\sqrt{F_{n+1}^2 + F_n^2}$. Note that the zone of nonequivalent shifts shrinks to a point in the quasiperiodic limit. The shift $\mathbf{t}_s = 0.5(1, 1, 1)z$ which places the center of the acceptance domain on the body-centered position of the

TABLE I. Structural characteristics of the rational approximants: number of vertices N_{ver} of PPL, number of basic structural units PR, OR, and composite units RD, number of atoms N_{at} , composition x , number of atoms with coordination Z , symmetry, and period of cubic symmetry a_n in Å for $a_R = 5.13$ Å [see Eq. (2)].

Approximant: τ_n	1/0	1/1	1/1	2/1	2/1	2/1
Shift of AD: $(2/z)t$		(0, 1, 1)	(1, 1, 1)	(0, 1, 1)	(0, 1, 1)	(1, 1, 1)
Overlaps of RD				No	Yes	
N_{ver}	8	32	32	136	136	136
N_{PR}	4	20	20	84	84	84
N_{OR}	4	12	12	52	52	52
N_{RD}	0	6	0	20	32	24
N_{at}	40	162	168	692	680	688
$N(\text{Al,Zn})$	32	98	128	444	384	424
$N(\text{Mg})$	8	64	40	248	296	264
x	0.8	0.605	0.762	0.642	0.565	0.61
$N(Z = 12)$	0	98	32	348	288	392
$N(Z = 13)$	32	0	96	96	144	32
$N(Z = 14)$	0	12	0	40	56	48
$N(Z = 15)$	0	12	0	40	80	48
$N(Z = 16)$	8	40	40	168	112	168
\bar{Z}	13.60	13.36	13.52	13.40	13.39	13.37
Symmetry	$Pa\bar{3}$	$Im\bar{3}$	$I2_13$			$Pa\bar{3}$
Period a_n	8.728	14.12	14.12	22.85	22.85	22.85

zone Z defines a special class of symmetrical models.⁴¹ They possess special self-similar scaling properties: perfect 12-fold vertices in the 3/2, 5/3, 8/5, ... approximants are exactly τ^3 rescaled 1/0, 1/1, 2/1, ... approximants, respectively. Note that the projection algorithm works only from $\tau \sim \tau_1 = 1/1$ onward, and the 1/0 approximant can be found only by rescaling the 3/2 symmetric approximant. Rescaling of the perfect 12-fold vertices of an approximant with $t \neq t_s$ does not provide a tiling. For more detailed discussion of the PPL's, we refer to the paper of Mihalkovič and Mraňko.⁴¹

For the icosahedral alloys of the Al-Zn-Mg class, the

Penrose tiling is decorated as proposed by Henley and Elser.³⁵ In addition to the PR's and OR's, a rhombic dodecahedron (RD) consisting of two PR's and two OR's is proposed as a composite structural unit. In the Henley-Elser decoration Al(Zn) atoms occupy all vertices and midpoints of all edges of the structural units. Two Mg atoms are placed along the trigonal axis in each PR, including the PR's inside the RD. A special decoration is proposed for the fourfold vertex inside a RD: four Mg atoms are placed on edges originating from the fourfold vertex. Altogether eight Mg atoms inside a RD form a slightly distorted hexagonal bipyramid. The distribution

TABLE II. Structural characteristics of the rational approximants: continuation of Table I.

Approximant: τ_n	3/2	3/2	3/2	3/2	5/3	5/3
Shift of AD: $(2/z)t$		(0, 1, 1)	(0, 1, 1)	(1, 1, 1)	(1, 1, 1)	(1, 1, 1)
Overlaps of RD		No	Yes	No	Yes	No
N_{ver}	576	576	576	576	2440	2440
N_{PR}	356	356	356	356	1508	1508
N_{OR}	220	220	220	220	932	932
N_{RD}	92	136	96	120	384	552
N_{at}	2924	2880	2920	2896	12380	12224
$N(\text{Al,Zn})$	1844	1624	1824	1704	7780	7000
$N(\text{Mg})$	1080	1256	1096	1192	4600	5224
x	0.631	0.564	0.625	0.588	0.628	0.573
$N(Z = 12)$	1556	1336	1600	1480	6660	6696
$N(Z = 13)$	288	464	224	318	1116	936
$N(Z = 14)$	184	240	192	190	792	806
$N(Z = 15)$	184	336	192	336	792	806
$N(Z = 16)$	712	504	712	568	3020	2980
\bar{Z}	13.39	13.38	13.38	13.40	13.39	13.38
Symmetry			$Pa\bar{3}$	$Pa\bar{3}$	$I2_13$	$I2_13$
Period a_n	36.97	36.97	36.97	36.97	59.82	59.82

of the Al and Zn sites over possible lattice sites is assumed to be random. The definition of the RD is not unambiguous. Each two neighboring OR's in Penrose tiling can be uniquely completed by two PR's to a RD. However, if three or more OR's are aligned around a common edge, this configuration of OR's allows overlapping of neighboring RD's (sharing one OR). The overlap is restricted if only each second pair of OR's defines a RD. If the overlaps are eliminated the number N_{RD} of RD's is reduced (in the quasiperiodic limit) by a factor of 0.6869 (Ref. 18). As isolated OR's are decorated relatively loosely, a higher number of RD's in the model yields a higher packing fraction. Since the shift t of the acceptance domain changes the configuration of PR's and OR's and hence the number of RD's, the choice of t has also a considerable influence on the stoichiometry of a quasicrystalline approximant. The number of atoms in a model may be expressed as $N(\text{Al,Zn})=4(N_{PR} + N_{OR}) - 5N_{RD}$, $N(\text{Mg})=2N_{PR} + 4N_{RD}$, where $N_{PR} = 4F_{3n+2}$ and $N_{OR} = 4F_{3n+1}$ are the numbers of PR's and OR's before grouping to RD's. Hence a higher number of decorated RD's yields a higher concentration of Mg atoms. The structural characteristics of our models of quasicrystals based on PPL approximants from 1/0 to 5/3 are compiled in Tables I and II.

III. INTERATOMIC FORCES FOR MULTICOMPONENT ALLOYS

Interatomic forces are calculated using pseudopotential perturbation theory. We use the optimized orthogonal-

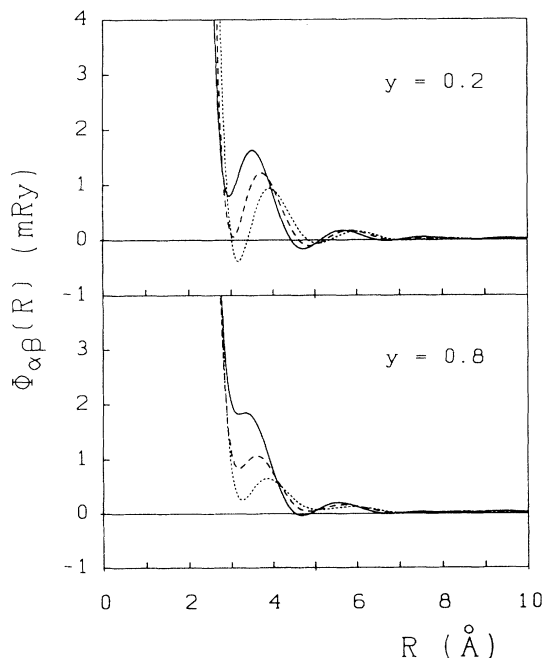


FIG. 1. Effective interatomic potentials $\Phi(R)$ in the quasicrystalline $(\text{Al}_y\text{Zn}_{1-y})_{0.625}\text{Mg}_{0.375}$ alloy for the compositions $y = 0.8$ and $y = 0.2$. Full line: Al(Zn)-Al(Zn) interactions; dotted line: Mg-Mg interaction; dashed line: Al(Zn)-Mg interaction.

plane-wave-based pseudopotential^{32,42} and the Ichimaru-Utsumi⁴³ local-field corrections to the dielectric function. For any details we refer to Refs. 32 and 42. For binary systems these pair potentials have been shown to be very realistic. For example, they have allowed us to discuss solid solubility and phase changes in crystalline Al-Mg alloys,³² to predict the structural energy difference between different Laves phase stacking variants of the compound MgZn_2 (Ref. 32), and to calculate accurate partial static and dynamic structure factors for glassy Mg-Zn alloys.⁵⁴ For simplicity the ternary alloy $(\text{Al,Zn})\text{Mg}$ is treated as a quasibinary system. We calculated two sets of interatomic potentials for the binary alloys $\text{Al}_x\text{Mg}_{1-x}$ and $\text{Zn}_x\text{Mg}_{1-x}$. For the ternary alloys $(\text{Al}_y\text{Zn}_{1-y})_x\text{Mg}_{1-x}$ the two sets of potentials are averaged in the ratio $y : (1 - y)$. Figure 1 shows the interatomic potentials for $(\text{Al}_y\text{Zn}_{1-y})_{0.625}\text{Mg}_{0.375}$ alloys for the compositions $y = 0.8$ and $y = 0.2$. The changes in the interatomic potentials with a varying Al/Zn ratio y (and hence with the electron/atom ratio which varies from $e/A = 2.45$ for $y = 0.8$ to $e/A = 2.11$ for $y = 0.2$) are rather small. Substitution of Al by Zn (and hence reduction of mean electron density) results in a smaller average diameter of X atoms and more attractive pair interactions. Nonetheless, our simulation studies show that this makes the difference between unstable and stable quasicrystalline alloys.

IV. MOLECULAR-DYNAMICS ANNEALING

The metastability of the idealized quasicrystalline structures was investigated using a simulated molecular-dynamics (MD) annealing at room temperature. The MD simulations were performed for the 1/0 to 5/3 approximants, i.e., for ensembles with $N = 40$ to $N = 12380$ particles in a periodically repeated cubic box. The simulations were performed in the microcanonical ensemble, temperature was controlled by a scaling of the velocities. Later MD runs were made in the canonical ensemble, using Nosé dynamics.⁴⁴ We found no essential differences in the microcanonical and canonical simulations. The Newtonian equations of motions have been integrated using a fourth-order predictor-corrector algorithm in the Nordsieck formulation,⁴⁵ with a time increment of $\Delta t = 0.5 \times 10^{-15}$ s. An effective network-cube algorithm was used for generating and storing the nearest-neighbor information.^{46,47} With this algorithm, the computer time increases only linearly with the number N of particles at a constant interaction radius. For further details, see, e.g., Ref. 48. For the lowest-order approximants, the potential was truncated at the largest distance compatible with the minimum image convention, $R_{\text{cut}} \approx 7.00$ Å. For the larger models, the cutoff was extended to $R_{\text{cut}} \approx 11.50$ Å. This means that in the smaller models each atom interacts with about 65 neighbors. In the largest models, the interaction-sphere contains nearly 300 atoms. Hence the sum over the damped oscillatory part of the pair potential should be well converged. To extend the interaction radius beyond the upper limit set by the minimum image convention could lead to a dis-

tortion of the structure which would be more serious than that caused by the unavoidable cutoff. Between 5000 time steps (for the largest model) and 20 000 time steps (for the smallest model) were used for production runs. The structure was controlled by calculating partial pair correlation functions, bond-angle distributions, and bond-angle correlation functions.

A structure was considered to be metastable if the potential energy and the partial correlation functions showed no systematic drift over the entire production run. Of course the MD simulation alone does not allow us to distinguish between stability and metastability. Stability can only be discussed with respect to competing phases, but of course it is quite impossible to calculate the enthalpies of all possible competing crystalline and amorphous phases.

V. STABILITY OF QUASICRYSTALLINE LATTICES UNDER REALISTIC PAIR FORCES

Our first task is to test the stability of the idealized structure model in the dependence from the interatomic forces, and hence from the electronic properties. We performed MD studies for the 3/2 approximant with $t = 0.5(1, 1, 1)z$ and no overlapping RD's. The vector t and the decoration of the rhombic dodecahedra were chosen such that the composition $(Al_y Zn_{1-y})_{1824} Mg_{1096}$ ($x = 0.625$) comes close to the $(Al, Zn)/Mg$ ratio of the observed icosahedral alloy.⁴⁹⁻⁵¹ The Al/Zn ratio was changed from $y = 1$ to $y = 0$ in steps of 0.2. Figure 2 shows the partial pair correlation functions after MD relaxation into equilibrium. We find that for $y = 1.0$ and $y = 0.8$ the room-temperature annealing leads to an amorphous state, hence the quasicrystal is clearly unstable. For $y = 0.6$ we find an intermediate state with at least some medium-range order. For $y \leq 0.4$ we find that the quasicrystalline long-range order is at least metastable, this is clearly reflected in the long-range oscillations in the partial pair distribution functions. The stable composition corresponds to electron-per-atom ratios of $e/A \approx 2.1-2.2$, in accordance with the experimental evidence that s, p -bonded icosahedral alloys have an electron concentration range $e/A \approx 2.1-2.4$ (Refs. 19-23) and the best single-phase icosahedral crystals are obtained at the composition $Al_{17}Zn_{32}Mg_{32}$ (Refs. 51 and 52).

An exhaustive discussion of the metastability or stability would require a calculation of the enthalpies and chemical potentials of all possible competing crystalline phases or phase mixtures. In our case we find that the quasicrystal is stable with respect to the pure metals. However, as the crystalline Frank-Kasper (FK) phase and the rational approximants to the quasicrystal have slightly different compositions, it is not meaningful to compare their energies directly. In this case stability of the quasicrystal requires that it has a lower energy than the mixture of the FK phase and a neighboring crystalline phase that has the same composition as the quasicrystal. It is clear that such calculations that are equivalent to a theoretical calculation of at least a part of the ternary phase diagram exceed by far the scope of the present

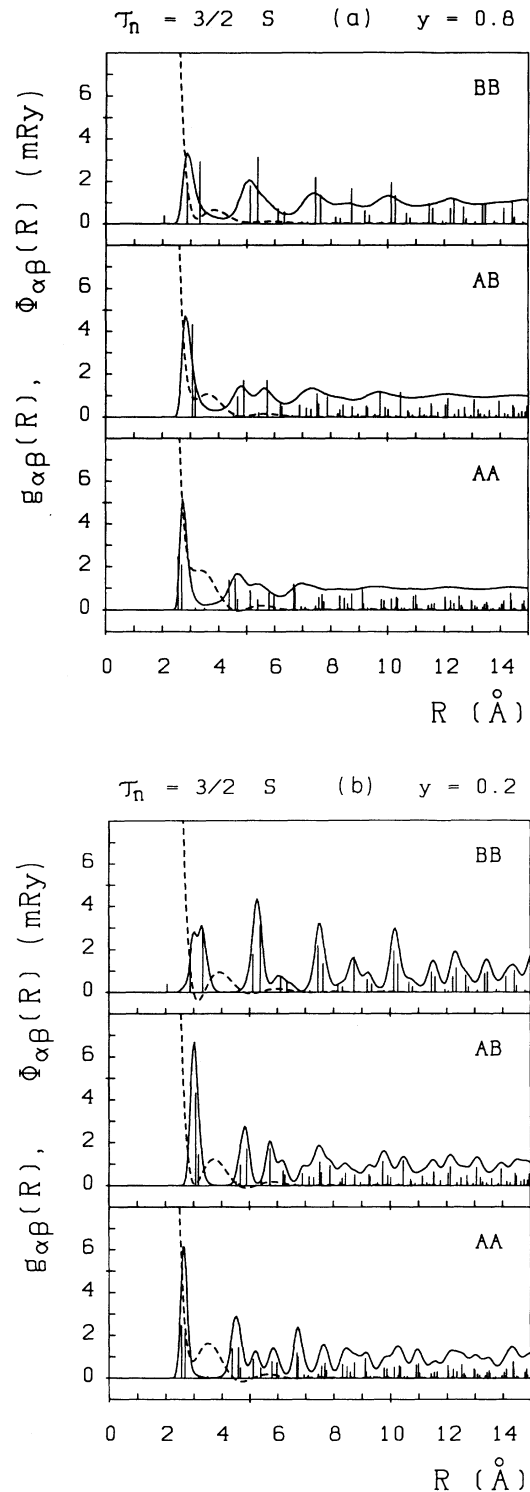


FIG. 2. Comparison of the interatomic potentials (dashed lines) with the partial pair correlation functions $g_{\alpha\beta}(R)$ (full lines) for the 3/2 approximant of the icosahedral $(Al_y Zn_{1-y})_{0.625} Mg_{0.375}$ phase with $y = 0.8$ and $y = 0.2$ after MD annealing at room temperature [A stands for Al(Zn), B for Mg atoms]. For $y = 0.8$ the icosahedral alloy relaxes to a glassy phase, for $y = 0.2$ the icosahedral alloy is found to be stable (cf. text). The vertical lines represent the interatomic distances (with heights proportional to their frequencies) for the ideal structure of the 3/2 approximant.

work. However, in the present context it is sufficient to establish the metastability of the quasicrystal by a MD simulation.

Figure 2 also compares the interionic distances of an ideal $3/2$ lattice with the pair interactions. For the Al-rich alloy, the closest Al(Zn)-Al(Zn) distance falls high on the steeply repulsive slope of the potential. This leads to a relaxation into a random-close-packed structure, even though the remaining interatomic distances are rather well adapted to the interatomic potentials. At a reduced Al content, a minimum exists in the Al(Zn)-Al(Zn) potential close to the quasicrystalline nearest-neighbor distances and this stabilizes the structure. Note that the appearance of this minimum is related to the reduction of the mean electron density and the ensuing reduction in the screening. At this composition the distance between the first- and the second-neighbor shells is close to the Friedel wavelength $\lambda_F = 2\pi/2k_F$, so that the atomic arrangement in the quasicrystalline structure is energetically favorable even for the interactions with the more distant neighbors.

This is precisely where the electronic factor appears: the Friedel wavelength depends on the electron density, and the matching of the interatomic distances d and the Friedel wavelength λ_F of the pair interactions is possible only at a certain value of the electron-per-atom ratio that depends on the geometrical properties of the structure under consideration. The criterion $d \approx \lambda_F$ is precisely a real-space formulation of Hume-Rothery criterion⁵³ for the stability of an electron compound. It has also been shown that a similar argument applies to the stability of an amorphous metallic alloys.⁵⁴ The q -space formulation of this criterion asks for $|\mathbf{Q}| \approx 2k_F$ (where \mathbf{Q} is a reciprocal-lattice vector) and the existence of a structure-induced minimum in the electronic density of states. In this form the existence a Hume-Rothery-like mechanism for stabilizing quasicrystals has been claimed by different groups,^{19–23} and the existence of the density-of-states minimum at the Fermi level has been demonstrated, at least for the lowest-order crystalline approximants.^{24–27} Figure 3 shows the diffraction

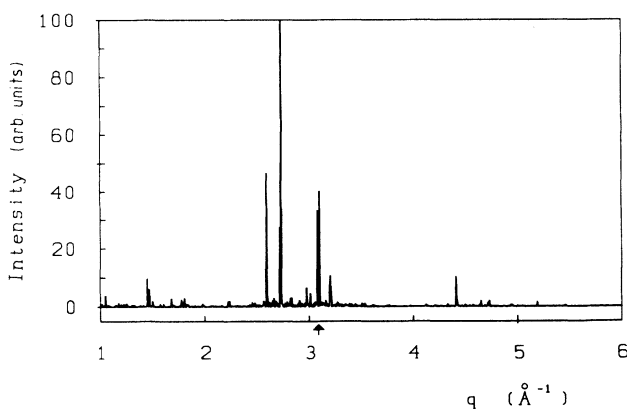


FIG. 3. X-ray-diffraction diagram for the relaxed $3/2$ approximant of Al-Zn-Mg. The arrow marks the diameter $2k_F$ of the Fermi sphere.

pattern of the relaxed $3/2$ approximant. We find that the Bragg peak corresponding to the (111101) reflection of the quasiperiodic phase agrees well with the diameter $2k_F$ of the Fermi sphere. Thus our molecular-dynamics results are in accordance with the conventional interpretation of the Hume-Rothery rules.

The MD studies also show that the annealing leads to a displacive modulation of the idealized structure, although it preserves the long-range order. In the following sections this modulated structure is investigated in detail.

VI. DISPLACIVELY MODULATED QUASICRYSTALS

The PPL's with Henley-Elser decoration represent idealized structures. The $1/1$ approximant corresponds to an idealized structure for the $(\text{Al,Zn})_{49}\text{Mg}_{32}$ Frank-

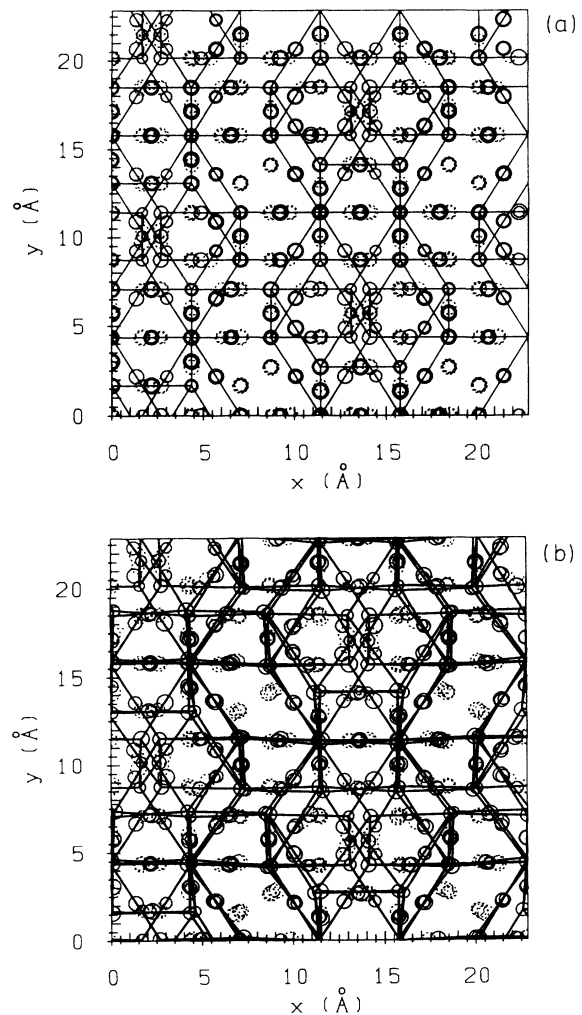


FIG. 4. Projection of the atomic positions in a $2/1$ approximant on an (x,y) plane. (a) Ideal structure, (b) displacively modulated structure. Full circles represent Al(Zn) atoms, broken circles represent Mg atoms. The size of the circles is scaled with the z coordinates. The straight lines show the edge of the Penrose tiles.

Kasper phase.^{36,55} For the real structure the rms deviations from the ideal locations are for Al(Zn) atoms 0.24 Å and 0.18 Å (sites on vertices and edges, respectively) and for Mg atoms 0.25 Å. Similar deviations are to be expected for the higher-order approximants and for the quasicrystal, because each basic unit appears in a large number of different local environments. Hence *any* interatomic force field must lead to a modulation of the idealized structure.

Figure 4 shows a comparison of the idealized structure with the modulated structure resulting from a room-temperature MD annealing at the example of the 2/1 approximant. The 688 atomic sites are projected on the (x, y) plane, the size of the symbols representing the atoms is scaled with the z coordinate. The edges of the Penrose rhombohedra are also drawn. We see that the modulation results in small displacements from the idealized sites, without destroying the quasicrystalline lattice. In the following, we investigate the manifestation of these displacements in the pair correlation functions, in the bond-orientational order, and in the diffractograms.

A. Partial pair correlation function

The lowest-order 1/0 approximant is obtained by τ^3 rescaling of the symmetric 3/2 approximant with $\mathbf{t} = \mathbf{t}_s$. This structure is stable under the given set of interatomic forces (Fig. 5). However, the stoichiometry is relatively far from the ideal quasicrystalline composition and the structure shows a preferred heterocoordination, which is not observed in the Frank-Kasper phase or in the quasicrystal.

For the low-order approximants both the idealized structure and the displacive modulation depend quite sensitively on the shift \mathbf{t} of the acceptance domain, i.e., on the configuration of the basic structural units. For the 1/1 approximant there exist two different configurations of the basic structural units. Each configuration corresponds to a region of equivalent shifts of the acceptance domain in the zone Z . The symmetric approximant with $\mathbf{t} = \mathbf{t}_s$ has a relatively high Al(Zn) content, the structure is marginally stable, as indicated by the broad and overlapping peaks in the pair correlation

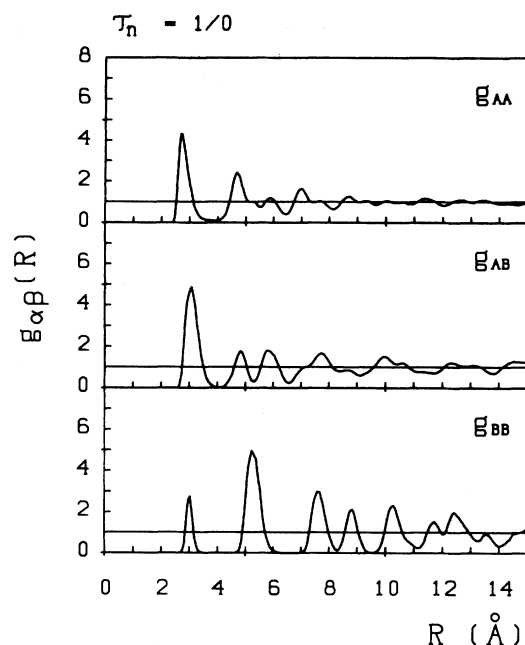


FIG. 5. Partial pair correlation functions $g_{\alpha\beta}(R)$ for the 1/0 approximant. $A = \text{Al(Zn)}$, $B = \text{Mg}$.

functions [see Fig. 6(a)]. The second configuration is the Frank-Kasper phase, which is obtained by a representative choice of, e.g., $\mathbf{t} = 0.5(0, 1, 1)z$. The Frank-Kasper phase is less strongly modified by the relaxation [see Fig. 6(b)], the displacive modulation is strongest for the Mg-Mg pair correlations, because the idealized structure contains some very short Mg-Mg distances which are incompatible with the Mg-Mg pair potential (cf. Fig. 2). The shortest Mg-Mg distances are those between the apices of the hexagonal bipyramids inside the rhombic dodecahedra. It is clear that the bipyramid can be elongated somewhat without breaking the local symmetry. In the bcc Frank-Kasper phase the Al(Zn) atoms at $(0, 0, 0)$ and $0.5(1, 1, 1)a$ have a fractional occupation probability (a is the lattice constant). If these Al(Zn) atoms are eliminated from the model, the widths of the peaks in

TABLE III. Comparison of the coordinates of atoms of the Frank-Kasper phase. The first column represents the notation for atomic positions (Ref. 35) with the number of equivalent positions. The second column lists the coordinates for an idealized decoration of the 1/1 periodic Penrose lattice, the third column the results of the molecular-dynamics calculation, and the last column those determined by diffraction studies (after Refs. 35 and 36).

	Ideal	Relaxed	Real
A2	(0.000, 0.000, 0.000)	(0.000, 0.000, 0.000)	(0.000, 0.000, 0.000)
C24	(0.000, 0.191, 0.309)	(0.000, 0.173, 0.318)	(0.000, 0.175, 0.301)
B24	(0.000, 0.096, 0.154)	(0.000, 0.099, 0.157)	(0.000, 0.091, 0.150)
F48	(0.154, 0.191, 0.404)	(0.163, 0.186, 0.405)	(0.168, 0.186, 0.403)
D16	(0.191, 0.191, 0.191)	(0.188, 0.188, 0.188)	(0.184, 0.184, 0.184)
E24	(0.000, 0.309, 0.118)	(0.000, 0.305, 0.119)	(0.000, 0.294, 0.119)
G12	(0.427, 0.000, 0.500)	(0.405, 0.000, 0.500)	(0.400, 0.000, 0.500)
H12	(0.191, 0.000, 0.500)	(0.201, 0.000, 0.500)	(0.180, 0.000, 0.500)

the Al(Zn)-Al(Zn) correlation functions is reduced: the rms deviations of the Al(Zn) vertex atoms from their idealized positions are 0.272 Å and 0.269 Å for the two models, respectively. For the Al(Zn) edge positions the corresponding numbers are 0.123 Å and 0.107 Å, for the Mg atoms, 0.157 Å and 0.163 Å. The atomic coordinates determined by the MD relaxation compare very well with the diffraction data for the Frank-Kasper phase³⁶ (Table

III). This confirms that our pair forces are indeed very realistic.

For the higher-order approximants the effect of a shift in the acceptance domain is gradually reduced. This is demonstrated in Fig. 7 with the example of the 2/1 approximants with $t = (0, 0, 0)$, $t = 0.5(0, 1, 1)z$, and $t = t_s = 0.5(1, 1, 1)z$. After the relaxation, there are only minimal differences in the correlation functions.

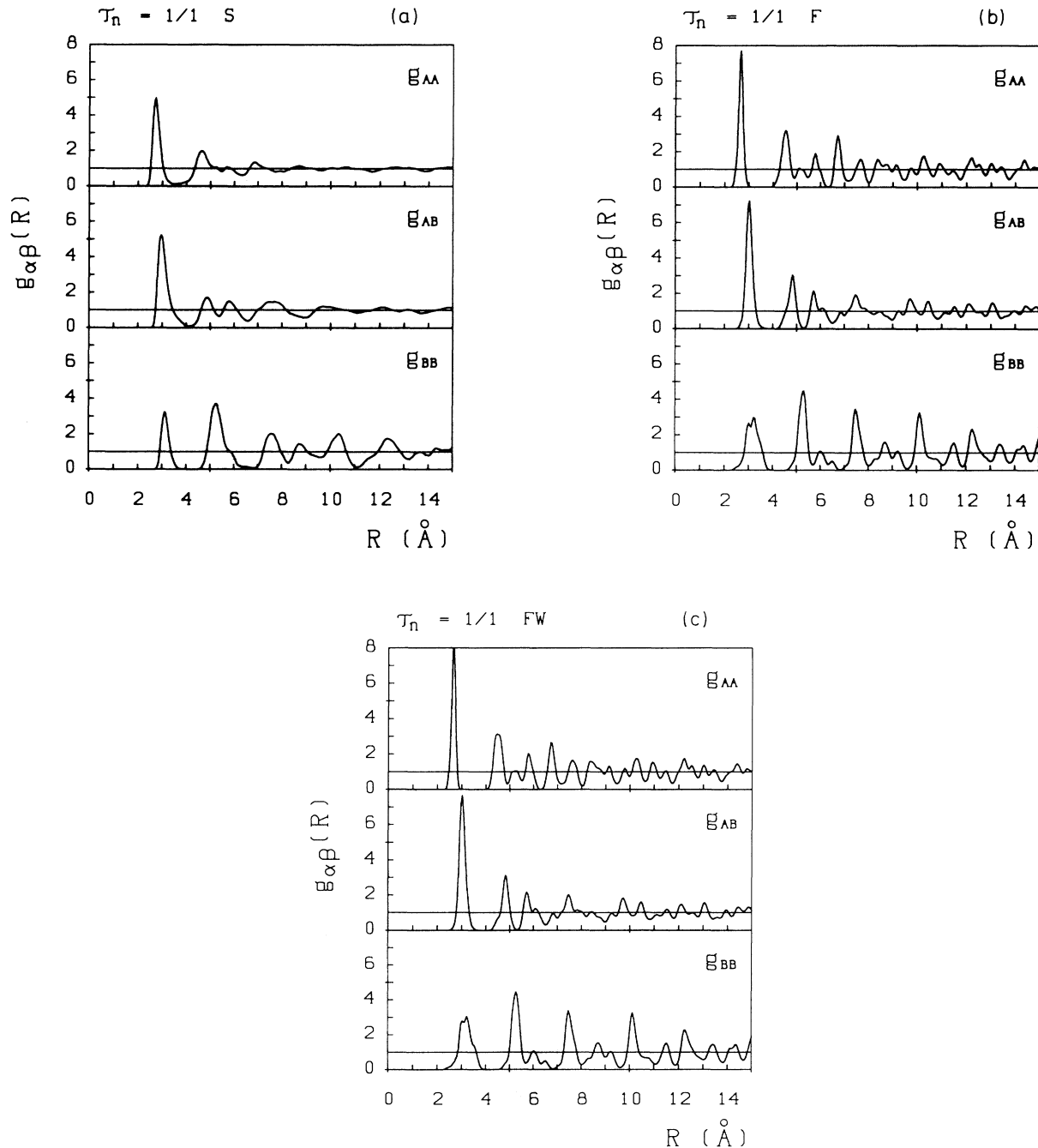


FIG. 6. Partial pair correlation functions $g_{\alpha\beta}(R)$ for different 1/1 approximants: (a) symmetric structure (label *S*) with $t = t_s = 0.5z(1, 1, 1)$; (b) $t = 0.5z(0, 1, 1)$, Frank-Kasper phase (label *F*); and (c) Frank-Kasper phase (label *FW*) with no Al atoms at $(0, 0, 0)$ and $0.5a(1, 1, 1)$.

The decision whether to allow for the overlapping of rhombic dodecahedra has a larger influence on the Al(Zn)/Mg composition and hence on the structure and the stability of the model. This is demonstrated in Fig. 8 for two variants of the 5/3 approximants with $t = t_s$ without and with overlapping RD's. With 12 380 [7780 Al(Zn) and 4600 Mg], respectively, 12 224 [7000 Al(Zn) and 5224 Mg] atoms in the cubic cell these are the largest models covered in our study. If overlapping of RD's is allowed, the relaxation leads to a considerably stronger

broadening and damping of the higher-order peaks in the $g_{\alpha\beta}$'s.

The observed broadening of the δ -function peaks of the idealized structures has a static and dynamic component, it is marginally larger for the best higher-order approximants than for the Frank-Kasper phase. The static displacements relative to the idealized structure are an intrinsic property of the decoration model for quasicrystalline structures: the locations of the atoms in the ideal

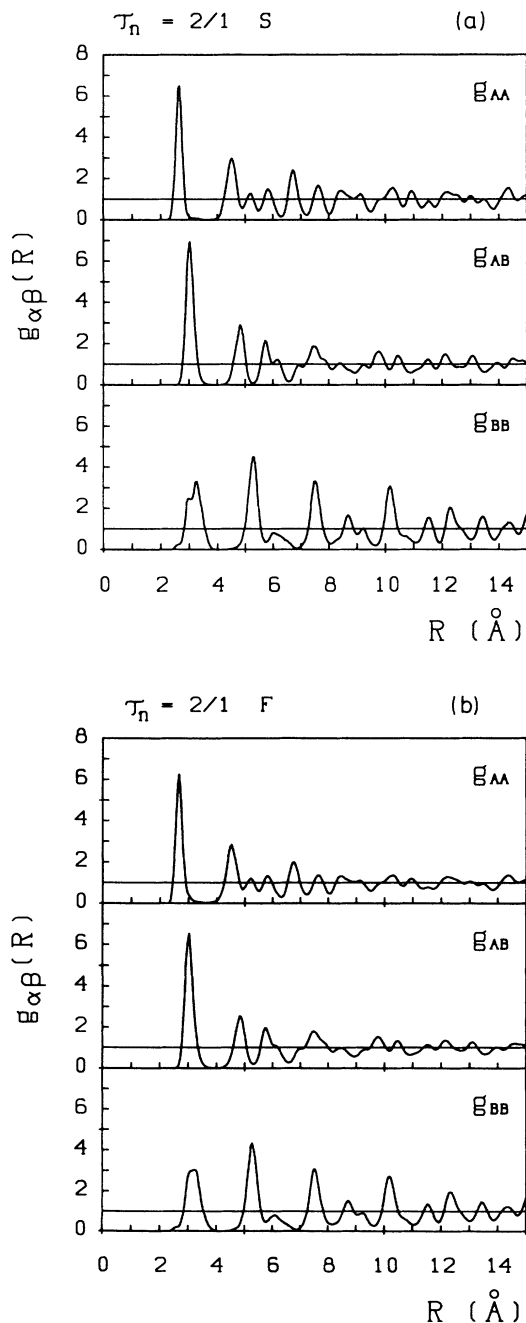


FIG. 7. Partial pair correlation functions $g_{\alpha\beta}(R)$ for different 2/1 approximants: (a) symmetric structure (S) with $t = t_s = 0.5z(1,1,1)$, (b) $t = 0.5z(0,1,1)$ marked (F).

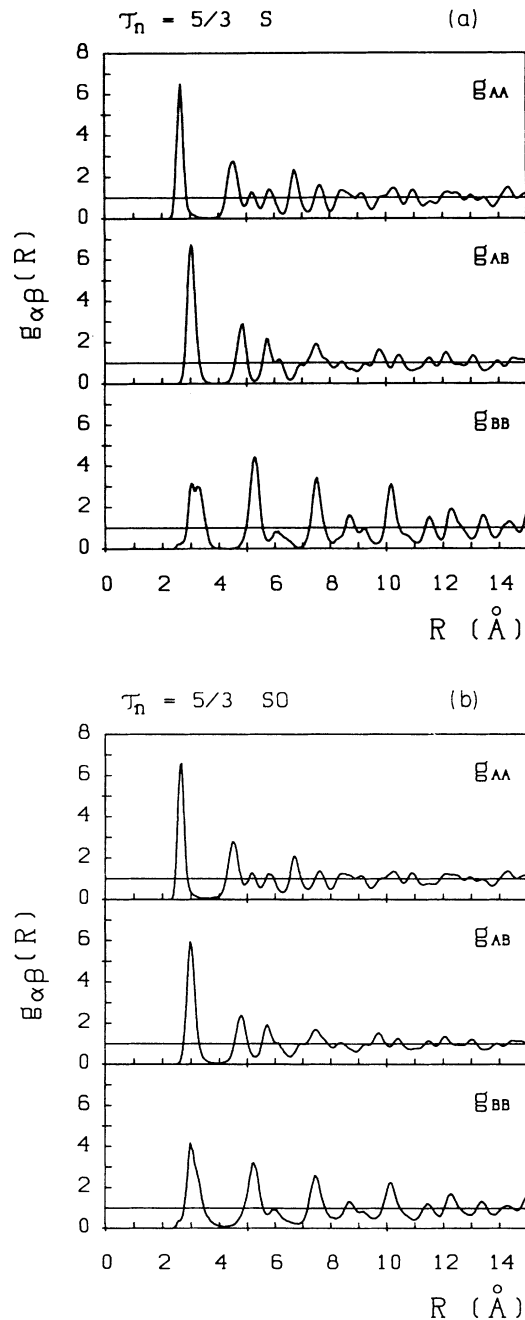


FIG. 8. Partial pair correlation functions $g_{\alpha\beta}(R)$ for the 5/3 approximant with $t = t_s$: (a) model S is decorated with no overlapping of rhombic dodecahedra (RD) and (b) model SO allows overlapping RD's.

lattice are solely controlled by the geometrical nature of the rhombohedral tiles and not by the overall environment of the atomic sites. The forces acting on the atoms of course depend on the global environment and hence yield static displacements which may be different for equivalent sites in different tiles. The point group symmetry however is not destroyed since the displacement field has the symmetry of the PPL. The result is what Jansen¹³ has called a displacively modulated quasicrystal.

The dynamic component of the displacement field is just the usual Debye-Waller broadening. Our result of a slightly larger broadening in the higher-order approximants to the quasicrystal than in the Frank-Kasper phase is in agreement with the observation of low-energy vibrational modes⁵⁶ in quasicrystals. Of course, the existence of low-energy modes is directly related to some degree of disorder.

B. Total pair correlation functions

The total pair correlation function may be measured in x-ray- or neutron-diffraction experiments on a polycrystalline or powdered sample. Since the interatomic distances in the Frank-Kasper phase and in the icosahedral differ only for $R \geq 10$ Å, the experiment has to be performed with a large range of momentum transfers to yield the necessary high resolution in r space.

Figure 9 shows the partial and x-ray-weighted reduced radial distribution function $G(R) = 4\pi nR[g(R) - 1]$ of the Frank-Kasper phase [1/1 approximant with $t = 0.5(0, 1, 1)z$], and the 5/3 approximant for distances up to 50 Å. For comparison we show on the same scale the experimental $G(r)$ of Mizutani *et al.*⁵⁷ for the Frank-Kasper and icosahedral phases. It is evident that in the computer simulation as well in the experiment the distribution functions of both phases are almost identical up to distances about 15 Å. In the range between 15 Å and 50 Å, the significant differences between the crystalline and the quasicrystalline phases are correctly reproduced by our model, even within details. The only difference is that the peaks in the simulated $G(R)$ are somewhat sharper. This is due to the fact that the resolution of the experimental $G(R)$ is still limited by truncation effects.

The almost perfect agreement of the theoretical model with experiment is to a large extent due to the displacive modulation of the idealized model. The results also show that by computer simulation as well as by experiment it will be very hard to differentiate between the higher-order approximants and the limiting quasicrystal.

It is expected that the model based on a Penrose lattice with Henley-Elser decoration applies not only to Al-Zn-Mg, but with minimal modifications to a wide class of the metastable (Al-Cu-Mg, Al-Zn-Li, Al-Ag-Mg, ...) (Refs. 58–62) and stable (Al-Cu-Li, Ga-Zn-Mg, ...) (Refs. 62–65) quasicrystals. Earlier attempts to use the Henley-Elser model to describe this class of alloys were considered at best partially successful.⁶⁰ However, these attempts were based on the idealized decoration. The obvious defect of the Henley-Elser decoration

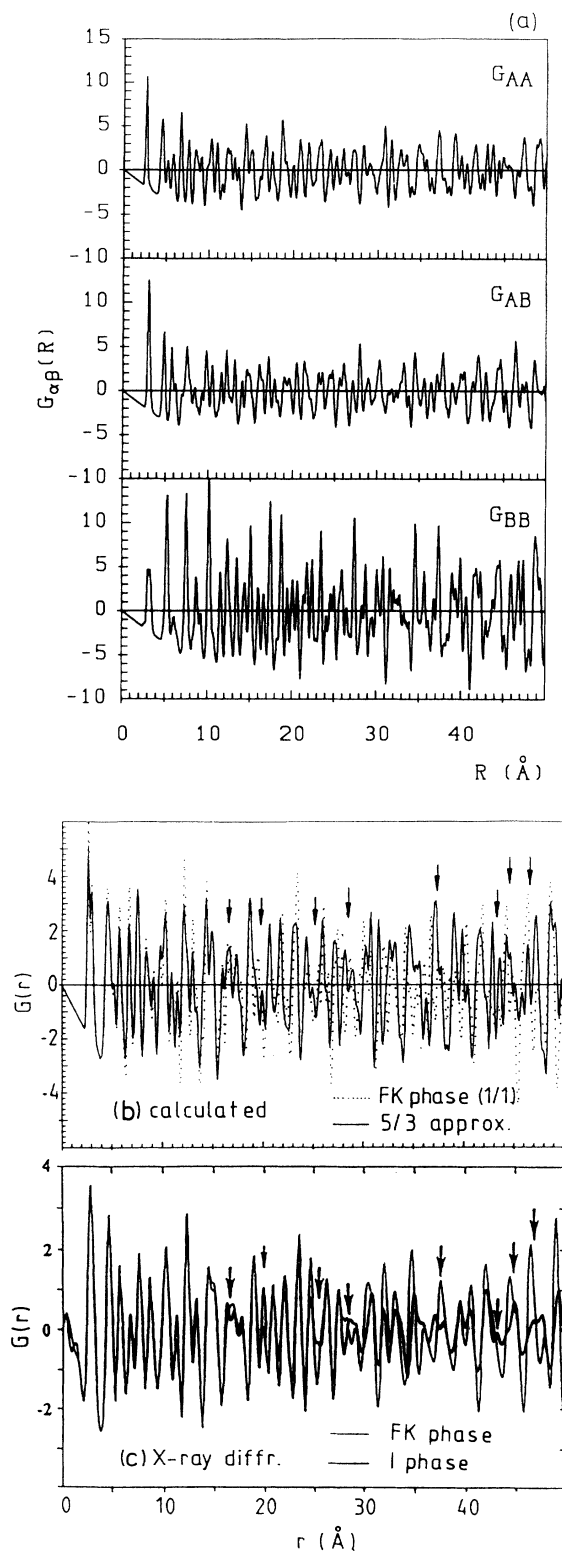


FIG. 9. (a) Partial and (b) and (c) x-ray-weighted reduced radial distribution function for the Frank-Kasper phase and the 5/3 approximant to the quasicrystalline structure, as obtained by molecular-dynamics relaxation (b), and for the Frank-Kasper and icosahedral phases as measured by Mizutani *et al.* (Ref. 57) (c).

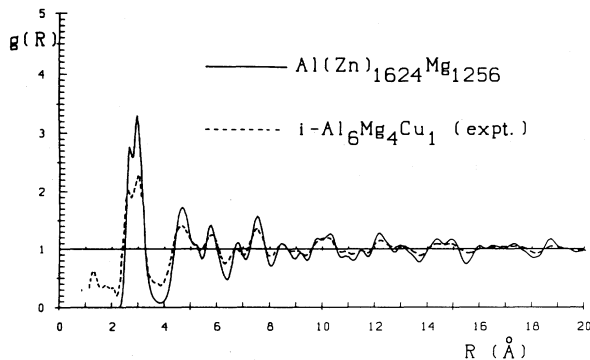


FIG. 10. Comparison of the x-ray-weighted pair correlation function $g(R)$ for $(\text{Al,Zn})\text{Mg}$ (3/2 approximant to the quasicrystal), full line, with the experimental result for icosahedral Al_6CuMg_4 (after Refs. 59 and 60), dashed line.

is the presence of short distances between two Mg atoms in RD's. This defect is, however, removed during MD annealing. A comparison of the present model for Al-Zn-Mg with the experimental results^{59,60} for Al-Cu-Mg (scaled to match the position of the first peaks) shows almost perfect agreement (Fig. 10). The displacive modulation of the structure is found to be very essential. This suggests that the relaxed Henley-Elser model is a satisfactory model of universal validity for the metastable quasicrystals of the Al-Zn-Mg class.

For the stable Al-Cu-Li quasicrystals, the Henley-Elser model was commented on rather critically.⁶⁶ Instead, models based on a decoration of large τ^3 -inflated Penrose rhombohedra with triacontahedral units have been proposed.^{64,66,67} The problem with these cluster-type models is that they define only about 80% of the sites of the quasilattice. The interstices between the triacontahedra remain ill-defined and have to be filled with "glue" atoms. Recently, we have been able to show that the Henley-Elser decoration may be modified to describe, after suitable MD annealing, the icosahedral structure of Al-Cu-Li.³⁴ It can also be shown that, at least on a local scale, the two models are not necessarily contradictory.

C. Bond-orientational order

The existence of long-range bond-orientational order is a distinguishing feature of quasicrystals. Orientational order is not independent of translational order. In crystals the existence of perfect translational order restricts the orientational order, in particular it excludes long-range icosahedral orientational order. In liquids thermal disorder restricts bond-orientational order to short distances. For supercooled liquids and glasses, computer simulations⁶⁸⁻⁷⁰ indicate the onset of long-range orientational order with icosahedral symmetry. The existence of noncrystallographic (i.e., icosahedral) bond-orientational order in liquids and small clusters has been discussed as early as 1952 by Frank.⁷¹ In the quasicrystals, icosahedral bond-orientational order coexists with quasiperiodic translational order.

Bond-orientational order may be characterized in various ways: on a local scale by the bond-angle distribution functions $f(\Theta)$ measuring the probability that two nearest-neighbor bonds around a given central atom form an angle Θ .⁷² On a global scale, bond-orientational order is characterized by the rotational invariants

$$Q_l = \left[\frac{4\pi}{2l+1} \sum_{m=-l}^l |Q_{lm}|^2 \right]^{1/2} \quad (3)$$

of the multipole moments

$$Q_{lm} = \langle Y_{lm}(\Theta, \phi) \rangle \quad (4)$$

of the directions of bonds relative to some fixed direction.⁷⁰ Θ and ϕ are the azimuthal and peripheral angles of a bond, Y_{lm} are spherical harmonics. The brackets symbolize an average over all bonds. We consider only the bonds between nearest-neighbor atoms. The nearest neighbors are defined from the condition that their distance is shorter than the distance to the first minimum after the main peak of the relevant partial pair correlation function $g_{\alpha\beta}(R)$. As in quasicrystals the first and second peaks are well separated (see Fig. 2), this definition is sufficiently accurate. Another common definition of nearest neighbors proceeds by the definition of Voronoi⁷³ or radical-plane polyhedra.⁷⁴ Especially for the large models, this is a very time-consuming calculation. For the close-packed alloys considered here, both definitions are almost equivalent.

Correlations between bonds at a distance R are described by the the bond-angle correlation function $G_l(R)$:⁷⁰

$$G_l(R) = \frac{4\pi}{2l+1} \sum_{m=-l}^l \langle Y_{lm}[\Theta(\mathbf{R}), \phi(\mathbf{R})] Y_{lm}[\Theta(\mathbf{0}), \phi(\mathbf{0})] \rangle. \quad (5)$$

\mathbf{R} is the vector connecting the center of gravity of the two bonds forming angles $\Theta(\mathbf{R}), \phi(\mathbf{R})$ and $\Theta(\mathbf{0}), \phi(\mathbf{0})$ relative to a fixed axis. The average is over all bonds at a fixed distance R .

1. Bond-angle distribution functions

Figure 11 shows that the main characteristics of the Frank-Kasper phase are preserved in the relaxed higher-order approximants: the Al(Zn) atoms occupy the centers of slightly distorted icosahedral coordination polyhedra, the Mg sites are coordinated in the form of Friauf polyhedra ($Z = 16$) and Frank-Kasper polyhedra ($Z = 14, 15$), see also Table I. Correspondingly, the bond-angle distributions around the Al(Zn) sites peak close to the bond angles of $\Theta = 63.5^\circ, 114.5^\circ$, and 180° corresponding to an ideal icosahedron, the bonds around the Mg atoms are distributed around the bond angles of the Friauf and Frank-Kasper polyhedra ($\Theta \sim 50^\circ - 63^\circ, 90^\circ - 100^\circ$, and $140^\circ - 145^\circ$). This distribution is hardly changed on relaxation and on going from the Frank-Kasper phase to the higher-order approximants. Note

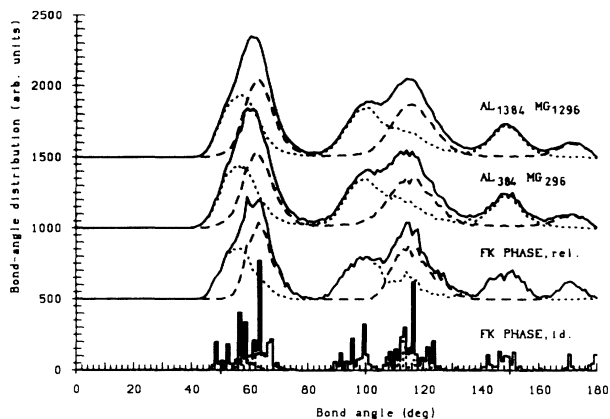


FIG. 11. Bond-angle distributions in the Frank-Kasper phase and in the higher-order approximants to quasicrystalline (Al,Zn)Mg. Full line: total distribution; dashed lines: around Al(Zn) sites with peaks close to the bond angles in an icosahedron; dotted lines: around Mg sites. See text.

that the distribution of the bond angles in the quasicrystalline model is similar, but more structured than that in amorphous alloys of comparable composition.⁷²

2. Invariants of bond directions

The bond-angle distribution functions measure the angles within a local coordinate system, the quadratic invariants Q_l characterize the orientation of the bonds relative to some fixed axis. The particular values for which nonzero spherical harmonics can occur depend only on the symmetry of the nearest-neighbor cluster: for icosahedral clusters only the spherical harmonics with $l = 6, 10, 12, \dots$ can occur,⁷⁰ cubic and hexagonal close-packed clusters have nonzero invariants also for $l = 4$ and $l = 8$. For the idealized models we find that the value of Q_6 is constant in the hierarchy of approximants,

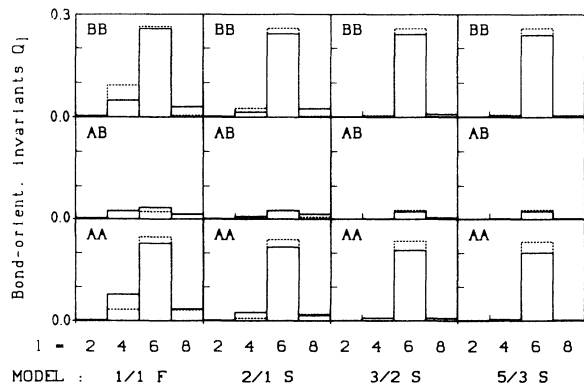


FIG. 12. Invariants Q_l of bond directions: evaluation of Q_l , $l = 2, 4, 6, 8$ in the hierarchy of crystalline approximants [A = Al(Zn), B = Mg]. Full lines: ideal configurations; dashed lines: relaxed configurations.

whereas Q_4 is strongly reduced relative to the Frank-Kasper phase (Fig. 12). For the largest model, only the icosahedral component of the bond-orientations survives. Upon relaxation, Q_6 is slightly reduced (indicating a certain smearing of the icosahedral correlations). This confirms that these models are predominantly icosahedrally oriented and that this is preserved on annealing.

3. Bond-angle correlation functions

Bond-angle correlation functions $G_l(R)$ have been first studied by Steinhardt, Nelson, and Ronchetti⁷⁰ for liquid and supercooled liquid Lennard-Jones systems. Steinhardt *et al.* measured the correlation functions by assigning each bond to a nearest vertex of a discrete mesh in the cubic MD box, the G_l 's are then calculated by three-dimensional fast-Fourier-transform techniques. The introduction of a cubic mesh leads to a coarse-grained sampling and a smoothed decay of the correlation functions with distance. We calculated the $G_l(R)$ by explicitly performing the average over all bonds within the model. Therefore the bond-angle correlation functions reflect the shell structure of the atomic packing. Figures 13 and 14 show the bond-angle correlation functions $G_6(R)$ and $G_4(R)$ for pairs of AA - AA, AA - BB, and

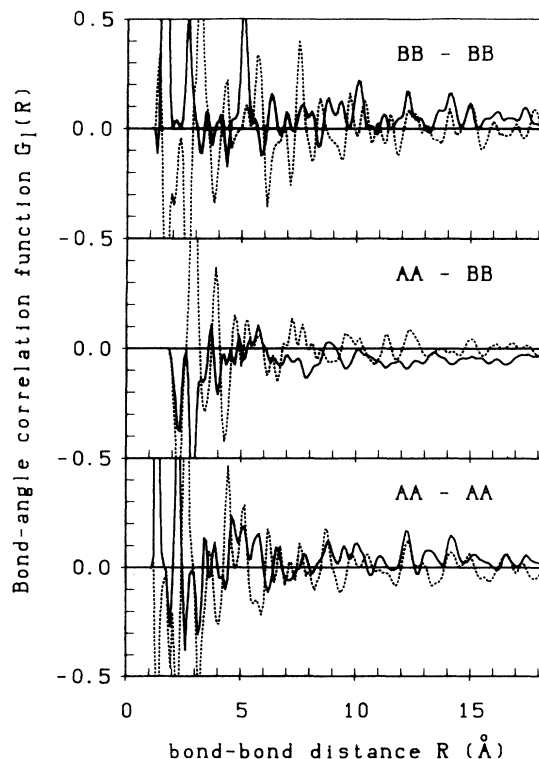


FIG. 13. Bond-angle correlation functions $G_l(R)$, $l = 4, 6$ for pairs (a) AA - AA, (b) AA - BB, and (c) BB - BB bonds [A = Al(Zn), B = Mg] in the 3/2 approximant to the quasicrystal. Note that $G_4(R)$ (dashed lines) oscillates at large R around zero, while $G_6(R)$ (full lines) oscillates around a nonzero value. This demonstrates the presence of the long-range icosahedral order.

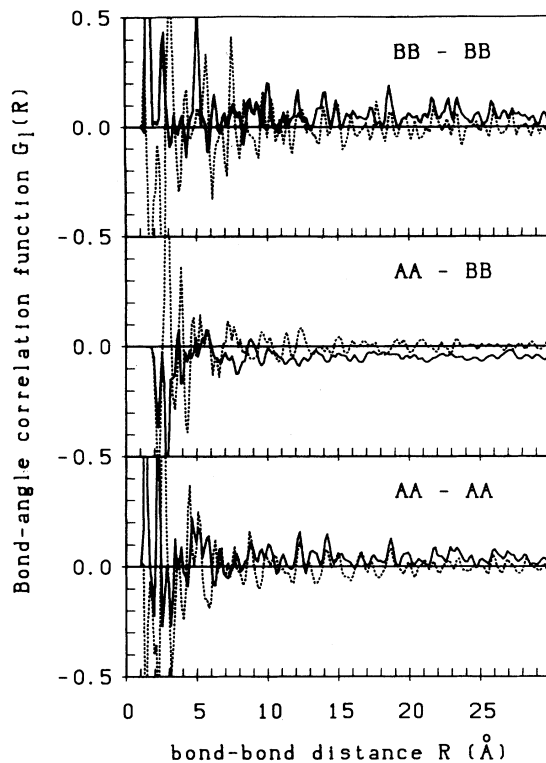


FIG. 14. Same as Fig. 13, but for the 5/3 approximant.

$BB - BB$ bonds [$A = \text{Al}(\text{Zn})$, $B = \text{Mg}$], calculated for 3/2 and 5/3 approximants of Al(Zn)-Mg quasicrystals. The $G_4(R)$ correlation functions reflecting a cubic symmetry in the bond-angle correlations decay very rapidly to zero. On the other hand, $G_6(R)$ remains nonzero even for the largest distances that can be realized within a given model. This demonstrates the existence of long-range icosahedral bond-orientational order.

D. Diffraction intensities

For a crystalline approximant, the diffraction intensities may be calculated directly from the known coordinates and occupation probabilities of atomic sites. The distribution of Al and Zn atoms in Al(Zn) sites was supposed to be uniformly random. With increasing order of the crystalline approximant, the Bragg reflections are more densely spaced, but the intensity is concentrated in a few dominant diffraction spots approaching the most important icosahedral reflections. The relaxation of the idealized structure leaves the positions of the Bragg reflections unchanged, but modulates their intensities. In Fig. 15 we compare the powder diffraction patterns of the ideal and relaxed approximants with those measured for the Frank-Kasper and the icosahedral phases.⁷⁵ We find that the position of the most intense Bragg peaks of the crystalline approximants converge very nicely towards the (100000), (110000), and (111101) diffraction peaks of the icosahedral phase. For the Frank-Kasper phase, the relaxation of the idealized structure turns out to be essential for achieving a good

agreement with the observed scattering intensities. For the higher-order approximants the effect of annealing on the diffraction pattern is not so evident. Of course, a really critical test of the structural model could be based only on a powder diffraction pattern with much better resolution.

It is also interesting to study the evolution of the single-

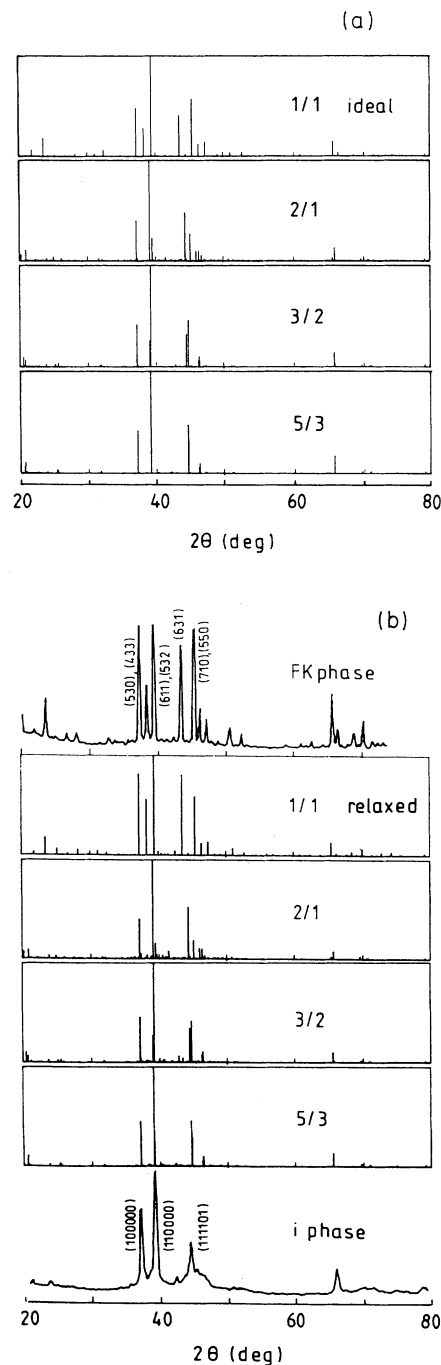


FIG. 15. X-ray powder diffraction patterns for the ideal (a) and relaxed (b) rational approximant of (Al,Zn)Mg, compared with observed scattering intensities of the Frank-Kasper and the icosahedral phases (after Ref. 75).

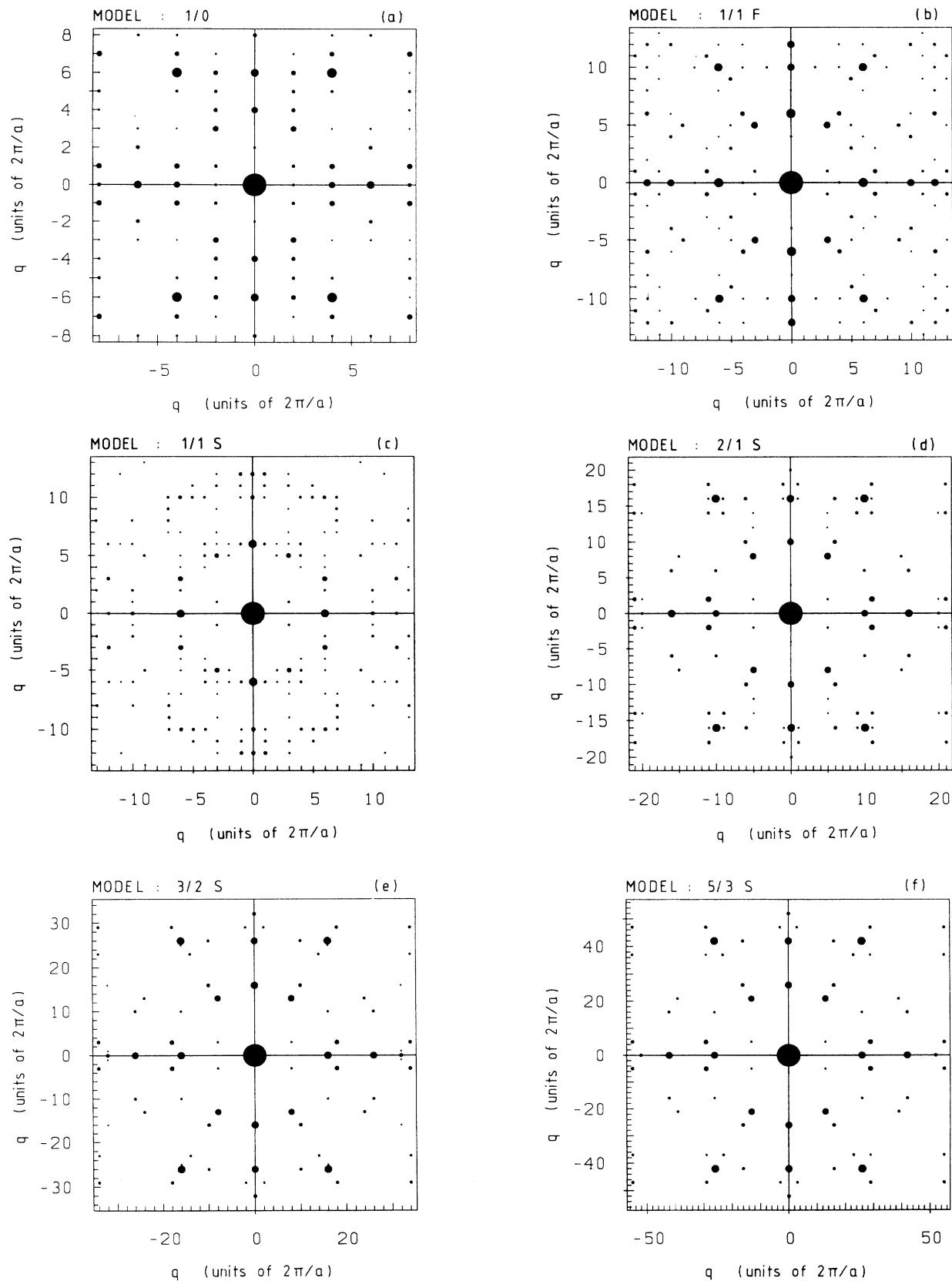


FIG. 16. X-ray diffraction in a plane perpendicular to a twofold axis, calculated for a series of relaxed crystalline approximants: 1/0, 1/1 F, 1/1 S, 2/1, 3/2, and 5/3 approximants. The size of the circles is scaled with the intensity of the diffraction spot, reflections with an intensity below the threshold 0.05 are not shown. The scale of $|q|$ is given in units $(2\pi/a)$, where $a = a_n$ is the period of cubic symmetry, see Tables I and II.

crystal diffraction patterns in the series of the approximants. Figure 16 shows the diffraction patterns in the [100] plane, i.e., in a plane perpendicular to a twofold axis of the quasicrystalline approximants and of the limiting quasicrystal. We find that as the period of the lattice is increased, the Bragg reflections are more densely spaced (they are dense everywhere in the quasiperiodic limit), but the scattering intensity is increasingly concentrated in the few characteristic Bragg spots corresponding to the main low-index Bragg reflections in the icosahedral phase. Note that the 1/0, 2/1, and 3/2 approximants with $t = t_a$ have space group symmetry $Pa\bar{3}$, so that in the (100) plane only reflections $(0kl)$ with $k = 2n$ (even) are allowed.

Unfortunately no single-crystal diffraction data are available for icosahedral Al-Zn-Mg. Also, the redistribution of the intensity in many closely spaced low-intensity peaks will hardly be observable experimentally. The modifications observed for the main diffraction peaks however are fully confirmed by the powder data.

VII. CONCLUSIONS

We have presented an investigation of the structure and stability of quasicrystalline alloys under realistic interatomic forces. The example chosen for our study is the icosahedral Al-Zn-Mg quasicrystal. We show that the quasicrystalline structure proposed for this system is stable only at the composition leading to an electron-per-atom ratio close to $e/A \sim 2.1 - 2.2$, a value which has been found to be characteristic for many quasicrystalline simple-metal alloys. The stability of the quasicrystalline phase is shown to depend on a constructive interference between the oscillations in the pair potentials and the interatomic distances. This requires that the Friedel wavelength of the potential λ_F corresponds to the interatomic distances d , i.e., $\lambda_F \approx d$. This condition is just the real-space formulation of a Hume-Rothery criterion for the electronic stabilization of a phase, $2k_F \approx |\mathbf{Q}|$, where \mathbf{Q} is the wave vector of a Bragg reflection. Thus our study extends and confirms recent arguments in favor of an electronically driven stability of quasicrystals formulated in terms of pseudogaps in the electronic density of states induced by the "quasi-Brillouin-zone"-Fermi-

surface interactions.¹⁹⁻²⁷

Any purely geometric description of a quasicrystal in terms of decorated Penrose tilings, as an icosahedral glass, or a random assembly of icosahedral clusters⁷⁶ is necessarily only a first approximation. In a quasicrystal, any atom is found in an infinite number of different environments (at least if the range of interaction is extended far enough). Hence the interatomic forces will lead to a displacive modulation of the idealized models. In our paper we present a detailed investigation of modulated tiling models. A modulated tiling is a quasiperiodic structure in which the atoms can be described as positions in a tiling and displacements such that the displacement field has the same symmetry as the tiling itself (or, more precisely, the displacement field has Fourier components belonging to the Fourier module of the tiling⁷⁷). Our results show that for a series of higher-order crystalline approximants the displacements induced by realistic interatomic forces conserve the symmetry of the model and improve the agreement with the observed pair correlation functions and diffraction patterns compared to earlier modeling studies based on idealized tiling models.

The results presented here refer to a metastable Al-Zn-Mg quasicrystal. Preliminary results³⁴ show that equally good fits can be achieved for the stable quasicrystals of the Al-Cu-Li class. Here again the displacive modulation is found to play a decisive role. Using interatomic forces based on tight-binding bond theory,^{78,79} it will be possible to extend these studies to quasicrystals of the Al transition-metal class.

Note added in proof. Recent results^{80,81} have shown that the modulated tiling models and the interatomic forces discussed in this paper provide an excellent basis for investigating the properties of vibrational excitations in quasicrystals of the Al-Zn-Mg and Al-Cu-Li classes.

ACKNOWLEDGMENTS

This work was supported by the Fonds zur Förderung der wissenschaftlichen Forschung (Austrian Science Foundation) under Project No. 8148-TEC. M.K. acknowledges a leave of absence from the Institute of Physics of the Slovak Academy of Sciences in Bratislava.

*On leave of absence from Institute of Physics, Slovak Academy of Sciences, CS-84228 Bratislava, ČSFR (permanent address).

¹D. Shechtman, I. Blech, D. Gratias, and J. W. Cahn, *Phys. Rev. Lett.* **53**, 1951 (1984).

²D. Levine and J. Steinhardt, *Phys. Rev. Lett.* **53**, 2477 (1984).

³D. Shechtman and I. Blech, *Metall. Trans. B* **16**, 1005 (1985).

⁴P. W. Stephens and A. I. Goldman, *Phys. Rev. Lett.* **56**, 1168 (1986).

⁵P. A. Heiney, P. A. Bancel, P. M. Horn, J. L. Jordan, S. La Placa, J. Angilello, and F. W. Galye, *Science* **238**, 660 (1987).

⁶M. V. Jaric, *Phys. Rev. Lett.* **55**, 607 (1985).

⁷P. Bak, *Phys. Rev. Lett.* **54**, 1517 (1984).

⁸N. D. Mermin and S. M. Troian, *Phys. Rev. Lett.* **56**, 2191 (1986).

⁹F. Lançon, L. Billard, and P. Chaudhari, *Europhys. Lett.* **2**, 625 (1986).

¹⁰F. Lançon and L. Billard, *J. Non-Cryst. Solids* **117+118**, 836 (1990).

¹¹Y. Sasajima, T. Miura, M. Ichimura, M. Imabayashi, and R. Yamamoto, *J. Phys. F* **17**, L53 (1987).

¹²M. Widom, K. J. Strandburg, and R. H. Swendsen, *Phys. Rev. Lett.* **58**, 706 (1987).

¹³T. Jansen, in *Quasicrystalline Materials*, edited by C. Janot and J. M. Dubois (World Scientific, Singapore, 1988), p. 327.

¹⁴P. W. Leung, C. L. Henley, and G. V. Chester, *Phys. Rev.*

- B **39**, 446 (1989).
- ¹⁵K. J. Szebo and J. Villain, Phys. Rev. B **36**, 4715 (1987).
- ¹⁶S. E. Burkov and L. S. Levitov, Europhys. Lett. **6**, 233 (1988).
- ¹⁷J. Roth, R. Schilling, and H. R. Trebin, Phys. Rev. B **41**, 2735 (1990).
- ¹⁸C. L. Henley, Phys. Rev. B **34**, 797 (1986).
- ¹⁹P. A. Bancel and C. L. Henley, Phys. Rev. B **33**, 7917 (1986).
- ²⁰J. Friedel and F. Denoyer, C. R. Acad. Sci. (Paris), Ser. II **305**, 171 (1987).
- ²¹V. G. Vaks, V. V. Kamysenko, and G. D. Samolyuk, Phys. Lett. A **132**, 131 (1988).
- ²²A. P. Smith and N. W. Ashcroft, Phys. Rev. Lett. **59**, 1365 (1987).
- ²³A. P. Tsai A. Inoue, and T. Masumoto, Sci. Rep. Res. Inst. Tohoku Univ., Ser. A **36**, 99 (1991).
- ²⁴T. Fujiwara, Phys. Rev. B **40**, 942 (1989); J. Non-Cryst. Solids **117+118**, 844 (1990).
- ²⁵T. Fujiwara and T. Yokokawa, Phys. Rev. Lett. **66**, 333 (1991).
- ²⁶J. Hafner and M. Krajčí, Europhys. Lett. **17**, 145 (1992).
- ²⁷J. Hafner and M. Krajčí, Phys. Rev. Lett. **68**, 2321 (1992); in *Physics and Chemistry of Finite Systems: From Clusters to Crystals*, edited by P. Jena, S. N. Khanna, and B. K. Rao (Plenum, New York, 1992), Vol. I, p. 587.
- ²⁸T. Tei, S. Takeuchi, and K. Kimura, J. Non-Cryst. Solids **117+118**, 769 (1990).
- ²⁹J. Hafner and M. Krajčí, Europhys. Lett. **13**, 335 (1990).
- ³⁰A. P. Smith, Phys. Rev. B **43**, 11 635 (1991).
- ³¹J. Hafner and V. Heine, J. Phys. F **13**, 2479 (1983); **16**, 1429 (1986).
- ³²J. Hafner, *From Hamiltonians to Phase Diagrams* (Springer, Berlin, 1987); in *The Structures of Binary Compounds*, edited by F. R. Boer and D. G. Pettifor (Elsevier, Amsterdam, 1989).
- ³³J. Hafner and G. Kahl, J. Phys. F **14**, 2259 (1984).
- ³⁴M. Windisch, *Diplomarbeit*, Technische Universität Wien, 1991; M. Windisch, M. Krajčí, and J. Hafner (unpublished).
- ³⁵C. L. Henley and V. Elser, Philos. Mag. Lett. **53**, 115 (1986).
- ³⁶G. Bergman, J. L. T. Waugh, and L. Pauling, Acta Crystallogr. **10**, 254 (1957).
- ³⁷J. E. S. Socolar, P. J. Steinhardt, and D. Levine, Phys. Rev. B **32**, 5547 (1985).
- ³⁸F. Gähler and J. Rhyner, J. Phys. A **19**, 267 (1986).
- ³⁹M. Krajčí and T. Fujiwara, Phys. Rev. B **38**, 12 903 (1988).
- ⁴⁰P. Bak, Phys. Rev. Lett. **56**, 861 (1986).
- ⁴¹M. Mihalkovič and P. Mrafko, J. Non-Cryst. Solids (to be published).
- ⁴²J. Hafner, J. Phys. F **5**, 1243 (1975).
- ⁴³S. Ichimaru and K. Utsumi, Phys. Rev. B **24**, 7385 (1981).
- ⁴⁴S. Nosé, J. Chem. Phys. **81**, 511 (1984).
- ⁴⁵C. W. Gear, *Numerical Initial Value Problem in Ordinary Differential Equations* (Prentice Hall, Englewood Cliffs, NJ, 1971), Secs. 9 and 10.
- ⁴⁶A. Arnold and N. Mauser, Comput. Phys. Commun. **59**, 267 (1990).
- ⁴⁷D. Finch and D. M. Heyes, in *Dynamical Processes in Condensed Matter*, edited by M. W. Evans (Wiley, New York, 1985), p. 493.
- ⁴⁸A. Arnold, N. Mauser, and J. Hafner, J. Phys.: Condens. Matter **1**, 965 (1989).
- ⁴⁹H. S. Chen, J. C. Phillips, P. Villars, A. R. Kortan, and A. Inoue, Phys. Rev. B **35**, 9326 (1987).
- ⁵⁰H. S. Chen and A. Inoue, Scr. Metall. **21**, 527 (1987).
- ⁵¹U. Mizutani, A. Kamiya, T. Matsuda, K. Kishi, and S. Takeuchi, J. Phys. CM **3**, 3711 (1991).
- ⁵²H. Yamane, K. Kimura, T. Shibuya, and S. Takeuchi, Mater. Sci. Forum **22-24**, 539 (1987).
- ⁵³W. Hume Rothery, *The Metallic State* (Oxford University Press, London, 1931).
- ⁵⁴J. Hafner and L. von Heimendahl, Phys. Rev. Lett. **42**, 386 (1980); J. Hafner, Phys. Rev. B **21**, 406 (1980); J. Phys. C **16**, 5773 (1983).
- ⁵⁵W. B. Pearson, *The Crystal Chemistry and Physics of Metals and Alloys* (Wiley, New York, 1972).
- ⁵⁶J. B. Suck, in *Quasicrystalline Materials*, edited by Ch. Janot and J. M. Dubois (World Scientific, Singapore, 1988), p. 337.
- ⁵⁷U. Mizutani, A. Kamiya, T. Fukunaga, and T. Matsuda, *Proceedings of the China-Japan Symposium on Quasicrystals* (World Scientific, Singapore, 1991).
- ⁵⁸G. V. S. Sastry, V. V. Rao, P. Ramachandrarao, and T. R. Anantharaman, Scr. Metall. **20**, 191 (1986).
- ⁵⁹Y. Sakurai, C. Kokubu, Y. Tanaka, Y. Watanabe, M. Masuda, and S. Nanao, Mater. Sci. Eng. **99**, 423 (1988).
- ⁶⁰Y. Sakurai, Y. Tanaka, Y. Watanabe, and S. Nanao, Phys. Rev. B **41**, 7377 (1990).
- ⁶¹W. Dmowski, T. Egami, Y. Shen, S. J. Poon, and G. J. Shiflet, Philos. Mag. Lett. **56**, 63 (1987).
- ⁶²Y. Shen, W. Dmowski, T. Egami, S. J. Poon, and G. J. Shiflet, Phys. Rev. B **37**, 1146 (1988).
- ⁶³C. A. Guryan, P. W. Stephens, A. I. Goldman, and F. W. Gayle, Phys. Rev. B **37**, 8495 (1988).
- ⁶⁴M. Audier, J. Pannetier, M. Leblanc, C. Janot, J. M. Lang, and B. Dubost, Physica B **153**, 136 (1988).
- ⁶⁵K. Edagawa, K. Suzuki, M. Ichihara, S. Takeuchi, A. Kamiya, and U. Mizutani, Philos. Mag. Lett. **64**, 95 (1991).
- ⁶⁶M. de Boissieu, C. Janot, J. M. Dubois, M. Audier, M. Jaric, and B. Dubost, in *Quasicrystals*, edited by M. Jaric and S. Lundquist (World Scientific, Singapore, 1990), p. 109.
- ⁶⁷M. Audier and P. Guyot, in *Quasicrystalline Materials*, edited by C. Janot and J. M. Dubois (World Scientific, Singapore, 1988), p. 181.
- ⁶⁸M. R. Hoare, J. Non-Cryst. Solids **31**, 157 (1978); Ann. N.Y. Acad. Sci. **279**, 186 (1976).
- ⁶⁹J. Farges, B. Raoult, and G. Tarchet, J. Chem. Phys. **59**, 3454 (1973).
- ⁷⁰P. J. Steinhardt, D. R. Nelson, and M. Ronchetti, Phys. Rev. B **28**, 784 (1983).
- ⁷¹F. C. Frank, Proc. R. Soc. London, Ser. A **215**, 43 (1952).
- ⁷²J. Hafner, J. Phys. (Paris) Colloq. **46**, C9-69 (1985).
- ⁷³R. Collins, in *Phase Transitions and Critical Phenomena*, edited by C. Domb and M. S. Green (Academic, New York, 1972), Vol. 2.
- ⁷⁴B. J. Gellatly and J. L. Finney, *Proceedings of the 4th International Conference on Rapidly Quenched Metals*, edited by T. Masumoto and K. Suzuki (The Japan Institute of Metals, Sendai, 1981), p. 275.
- ⁷⁵T. Rajasekharan, D. Akhtar, R. Gopalan, and K. Muraleedharan, Nature (London) **322**, 528 (1986).
- ⁷⁶J. L. Robertson and S. C. Moss, J. Non-Cryst. Solids **106**, 336 (1988); Z. Phys. B **83**, 391 (1991).
- ⁷⁷T. Jansen, Phys. Rep. **168**, 55 (1988).

⁷⁸Ch. Hausleitner and J. Hafner, Phys. Rev. B **42**, 5863 (1990).

⁷⁹Ch. Hausleitner and J. Hafner, Phys. Rev. B **45**, 115 (1992); **45**, 128 (1992).

⁸⁰J. Hafner and M. Krajci, Europhys. Lett. (to be published).

⁸¹J. Hafner and M. Krajci, in *Proceedings of the 8th International Conference on Liquid and Amorphous Metals* [J. Non-Cryst. Solids (to be published)].